

Biophysical Journal, Volume 118

Supplemental Information

**Nanoscale Heat Transfer from Magnetic Nanoparticles and Ferritin in an
Alternating Magnetic Field**

Hunter C. Davis, Sunghwi Kang, Jae-Hyun Lee, Tae-Hyun Shin, Harry Putterman, Jinwoo Cheon, and Mikhail G. Shapiro

Supplementary Information for “Nanoscale Heat Transfer from Magnetic Nanoparticles and Ferritin in an Alternating Magnetic Field”

Hunter C. Davis, Sunghwi Kang, Jae-Hyun Lee, Tae-Hyun Shin, Harry Putterman, Jinwoo Cheon, Mikhail G. Shapiro (mikhail@caltech.edu)

Supplementary Figures

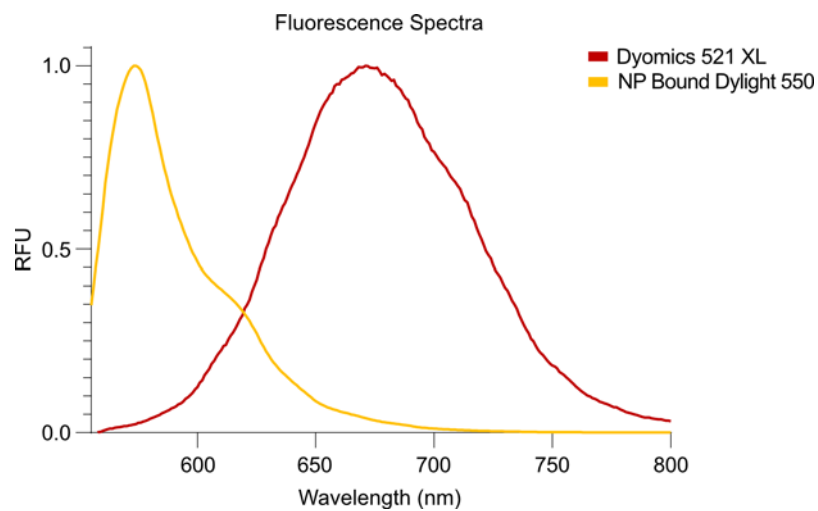


FIGURE S1. Fluorescence emission spectra of Dylight 550-conjugated nanoparticles (NP) and DY-521XL. Spectra were measured in a Molecular Devices spectrophotometer. Excitation was set at 532 nm.

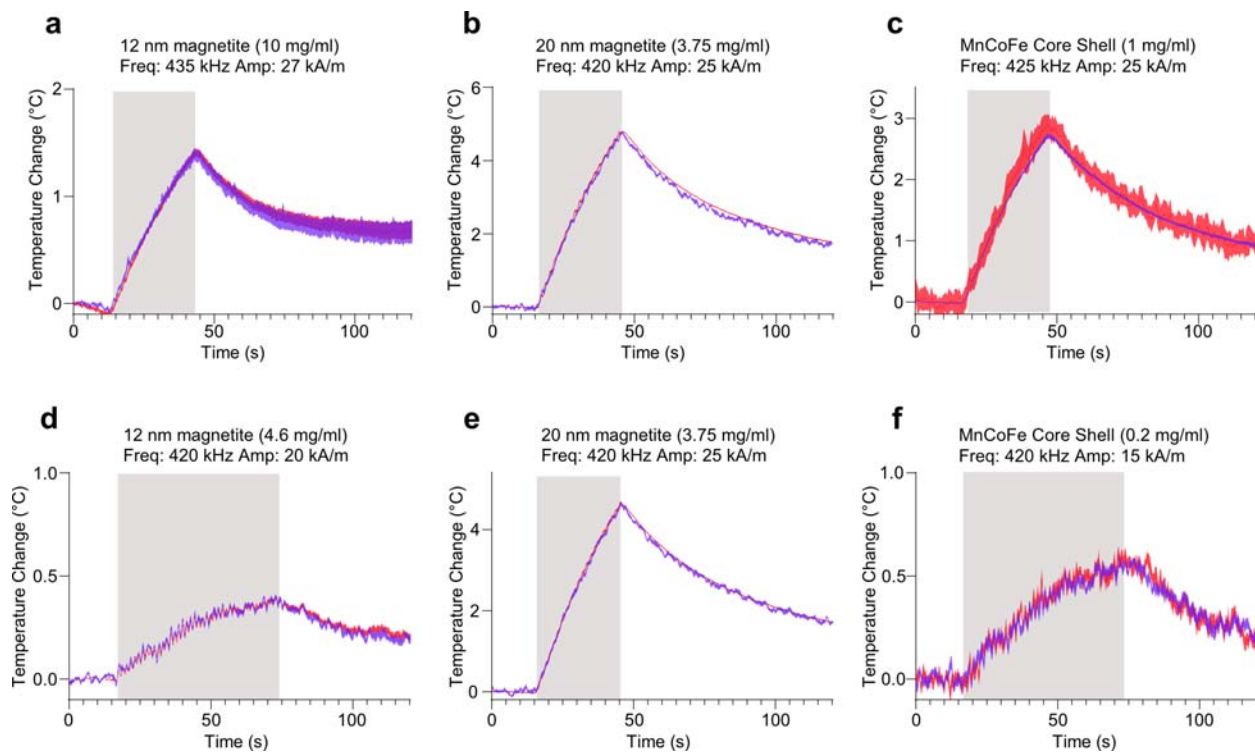


FIGURE S2. Additional hyperthermia trials with separate batches of magnetic particles. Surface and fluid temperatures measured for each nanoparticle type during RF-AMF application. Mean and SEM temperature for particle surface (red) and surrounding fluid (blue) are plotted for each sample, with frequency and field parameters specified above the plot. RF-AMF application period is denoted by grey shading. Each trace denotes the mean \pm S.E.M. of 20 runs of RF-AMF stimulation.

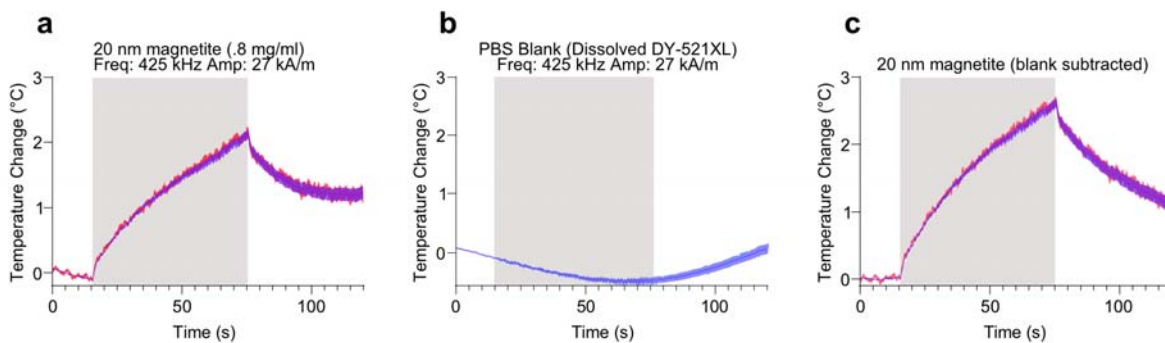


FIGURE S3. Artifact from background temperature variation due to the toroid. As stated in **Fig. 3** in the main text, our 400-700 kHz toroid did not completely cool in between stimuli, resulting in a slow apparent cooling at the beginning of the averaged plot. The ferrofluid easily reaches thermal equilibrium with its surroundings over the nine minutes between stimuli, such that this slow cooling behavior of the toroid should be identical irrespective of the presence of nanoparticles in the sample. (a) Thermometry of 20 nm magnetite nanoparticle ferrofluid during RF-AMF application from **Fig. 3d** (b) Thermometry of DY-521XL in PBS during RF-AMF application matching the field parameters in (a) establishes the background thermal variation of the sample due to the toroid. (c) Subtracting this background variation from the thermometry measurement of the ferrofluid under RF-AMF stimulus eliminates the slow cooling at the beginning of the trace. Mean and SEM temperature for particle surface (red) and surrounding fluid (blue) are plotted for each sample, with frequency and field parameters specified above the plot. RF-AMF application period is denoted by grey shading. Each trace denotes the mean \pm S.E.M. of 20 runs of RF-AMF stimulation.

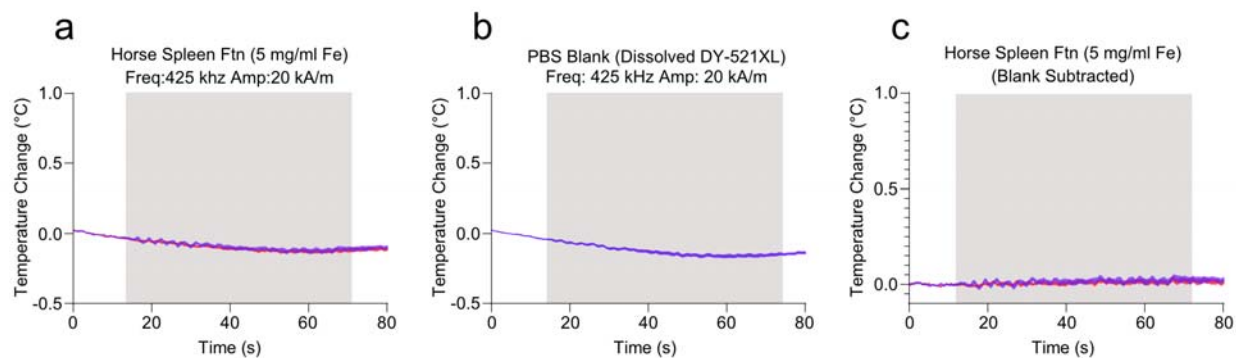


FIGURE S4. Background temperature variation in low frequency ferritin experiment. (a) Surface and fluid temperature of ferritin solution during RF-AMF application. Incomplete cooling of the toroid between stimuli leads to a slow cooling through RF-AMF stimulation in the ferritin ferrofluid. (b) Thermometry of DY-521XL in PBS during RF-AMF application matching the field parameters in (a) establishes the background thermal variation of the sample due to the toroid. (c) Subtracting background thermal variation from thermometry of ferritin under RF-AMF stimulation reveals no measurable heating from ferritin on the protein surface or in the surrounding fluid. Mean and SEM temperature for particle surface (red) and surrounding fluid (blue) are plotted for each sample, with frequency and field parameters specified above the plot. RF-AMF application period is denoted by grey shading. Each trace denotes the mean \pm S.E.M. of 20 runs of RF-AMF stimulation.

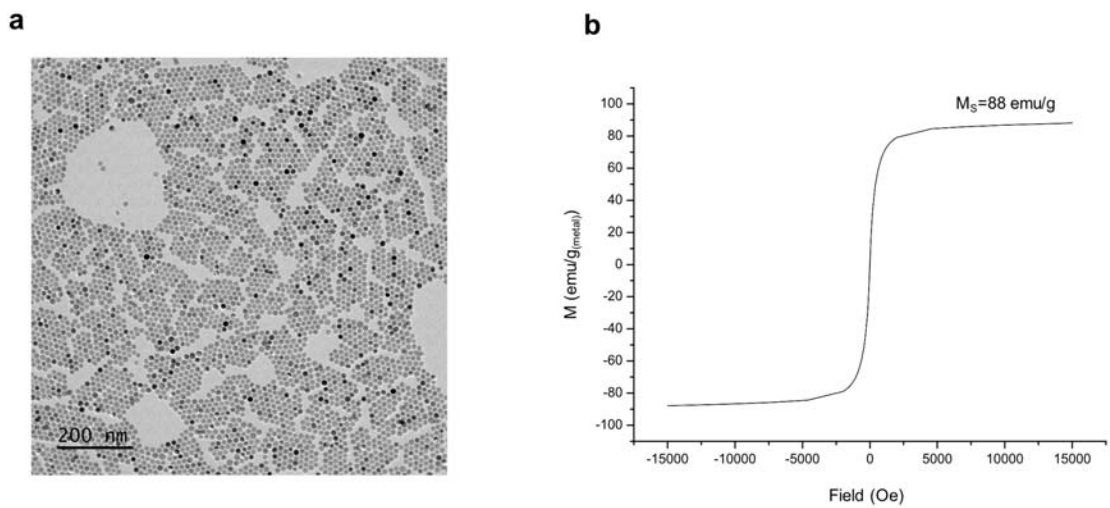


FIGURE S5. Characterization of core-shell nanoparticles. (a) Transmission electron microscope (TEM) image and (b) magnetic measurement of core-shell nanoparticles. TEM observation were made using the JEM-2100Plus (JEOL) under the acceleration voltage of 200 kV. Magnetic property was measured using vibrating sample magnetometer (Lake Shore Cryotronics, Inc.) and mass of metal was measured using inductively-coupled plasma optical emission spectroscopy (Thermofisher).

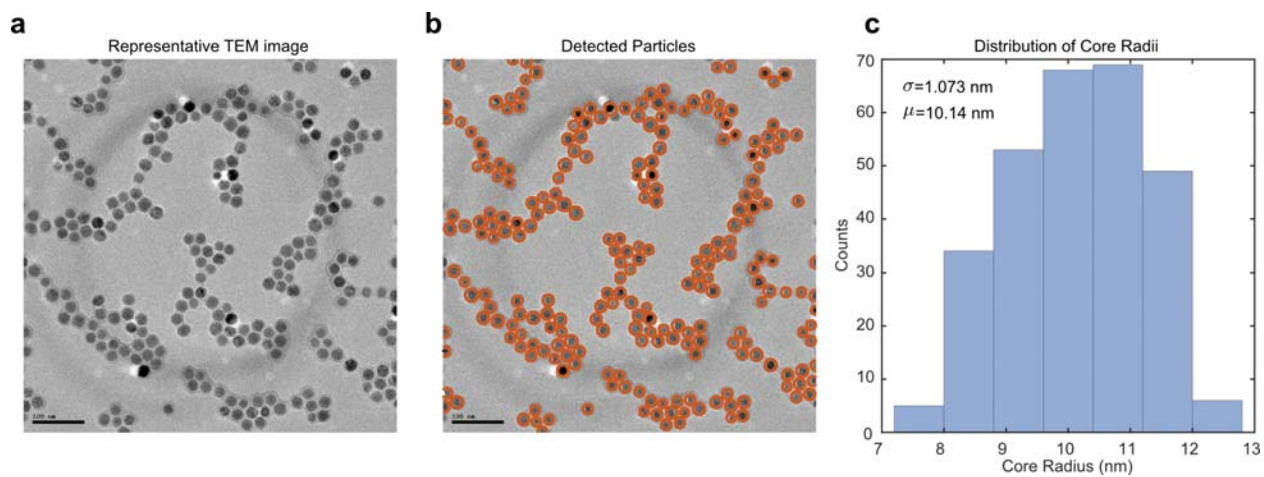


FIGURE S6. Size distribution of 20 nm magnetite nanoparticles. (a) Representative transmission electron microscope (TEM) image of SHA20 nanoparticles from Ocean Nanotech. (b) Particles detected and sized using a custom imaging processing script. (c) Distribution of particle radii taken from a total of 289 particles. Scale bar is 100 nm.

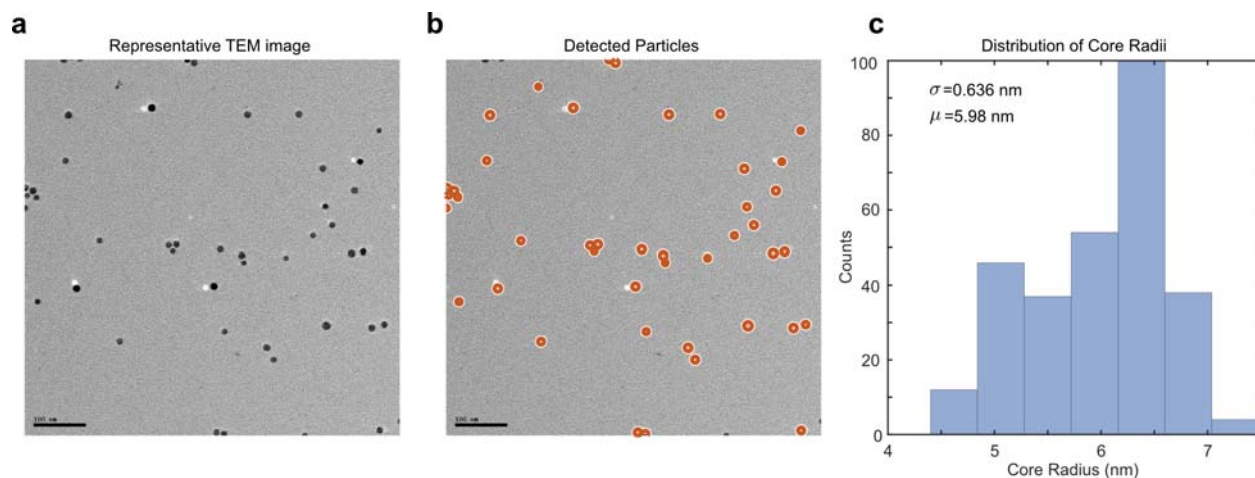


FIGURE S7. Size distribution of 12 nm magnetite nanoparticles. (a) Representative transmission electron microscope (TEM) image of SHA10 nanoparticles from Ocean Nanotech. (b) Particles detected and sized using a custom imaging processing script. (c) Distribution of particles radii taken from a total of 291 particles. Scale bar is 100 nm.

Supplementary Tables

	20 nm	12 nm	CS
Fraction D550 Signal in FT	0.181	0.003	0.089
Max Release Induced Error ($^{\circ}$ C)	0.005	<.001	0.009

TABLE S1. Error from dye release for 20 nm magnetite (20 nm), 12 nm magnetite (12 nm), and MnCoFe core-shell nanoparticles (CS). A small amount of nonspecifically bound Dylight 550 was released from the nanoparticle surface during stimulus. Due to the strong quenching of dye conjugated to the nanoparticle surface, this released Dylight 550 could account for a non-negligible fraction of the overall measured Dylight 550 fluorescence. In order to ensure that this did not confound our results, we measured the fractional contribution of released Dylight 550 to the overall Dylight 550 signal. We did so by separating the nanoparticle-bound dye from dissolved dye after completion of the standard RF-AMF stimulus (20 one-min stimuli at 420 kHz and 25 kA/m with 9 min in between stimuli) for each synthetic magnetic particle sample type using 10 kDa size exclusion filters (Amicon). The retentate was diluted with PBS to match the original particle concentration. An equivalent concentration of unlabeled nanoparticles was

added to the flow-through to account for the nanoparticle's optical attenuation. The fluorescence of the retentate and flow through (FT in table) were then measured at 570 nm (530 nm excitation) using a Molecular Devices spectrophotometer. Assuming the nanoparticle surface and surrounding fluid maintained two distinct temperatures, the overall Dylight 550 signal would be a weighted average of the two environments. As a result, it is possible to approximate the error induced by the released dye:

$$\text{Dylight Temp.} = (1 - \text{Released Frac.}) * \text{Surface Temp} + \text{Released Frac.} * \text{DY521 Temp.}$$

$$\text{Surface Temp.} = (\text{Dylight Temp.} - \text{Released Frac.} * \text{DY521 Temp.}) / (1 - \text{Released Frac.})$$

$$\text{Max Error} = \max\{\text{Surface Temp.} - \text{Dylight Temp.}\}$$

Here *Dylight 550 Temp.* is the Dylight 550 temperature measured in our fluorometer during RF-AMF application, *Released Frac.* is the fraction of the total D550 signal in the flow through after size-exclusion filtration, *DY521 Temp.* is the DY-521XL temperature measured during RF-AMF application, and *Surface Temp.* is the actual temperature at the nanoparticle surface.